Computational methods in engineering sciences, vol. 1, no. 4, Winter 2024 Serial no. 4
DOI: 10.22034/cmes.2024.2024131.1022

The effect of curves of tangential channel on gas cyclone performance

F. Parvaz [1, *]

[1] Department of Mechanical Engineering, Semnan University, P.O. Box 35131-191, Semnan, Iran
* Corresponding Author

Received: 02/01/2024, Revised: 29/02/2024, Accepted: 10/03/2024.

Abstract
Gas separators have many different applications to separate and classify solid particles from the continuum phase. The geometry of the separator is the key part that is able to improve collection efficiency. This study considers the impact of the curve degree located at the end of the channel of a gas cyclone on the flow pattern and the performance gas cyclone. The usage of Computational fluid dynamics (CFD) in separators with different curves was conducted using the turbulent model of Reynolds Stress Modeling (RSM). To obtain the distribution of particles, Eulerian-Lagrangian is used in all gas cyclones. The obtained results illustrate that increasing inlet velocity can increase pressure drop and collection efficiency. By installing a curve at the end of the tangential channel, negative pressure at the central is less than wall regions. In addition, the tangential velocity pattern is symmetric, and maximum tangential velocity is almost 1-to-2-time inlet velocity and the maximum axial velocity is inside the exit tube.

Keywords
CFD, RSM, Gas cyclone, Curves channels.

1. Introduction
Cyclone separators or Aero-cyclones have been widely used in industrial applications [1], such as chemical processes and food drying. This device is popular among researchers and engineers due to its small size, low cost, and easy launching. In gas cyclones, the continuing phase (AIR) enters the inlet channel tangentially inside the cylindrical part. Due to the conical and cylindrical parts of the gas cyclone, it is a high swirl flow that causes turbulent gas flow. Numerical works have been carried out by many researchers who evaluate gas cyclone performance with geometrical changes. Gao et al.[2] have investigated the effect of central tubes in oil-gas cyclones. They reported that the effect of diameter is higher than high on gas flow. Raoufi et al.[3] studied the different shapes of vortex finder in a stairmand gas cyclone. They observed that decreasing the diameter of the vortex finder can cause the development of tangential velocity and collection efficiency, however, pressure drop increases. Brar et al.[4] studied the effect of outlet tube diameter on flow pattern. They found that decreasing diameter can cause an improvement in collection efficiency. Parvaz et al.[5] have studied the impact of eccentricity on gas cyclone performance. They reported that eccentricity can cause an unstable vortex inside a gas cyclone to decrease collection efficiency. Parvaz et al[6] numerically studied the effect of outlet shapes. They found that the maximum axial velocity was at the outlet tube of the diamond, but the minimum tangential velocity was at the outlet tube of the diamond. Parvaz et al[7] have studied the effect of varied shapes of vortex finders. They found that the shape of the vortex finder can impact gas cyclone performance. Qian and Wu[8] and Qian and zhang[9] studied the effect of inlet angle on gas performance. They have observed that 45 degrees compared with other angles have better collection efficiency. Safikhani et al[10] numerically investigated the number of inlet channels of a new design cyclone. They showed the three inlets can cause collection efficiency to increase more than one inlet and two inlets. Liu et al.[11] experimentally studied the impact of varied particle arrangements that are placed in the middle of tangential channels. They found out that increasing the flow rate increases pressure drop. Nihan et al.[12] have investigated the impact of the shape of the inlet cross-section. They proposed that a rectangular shape can result in higher and lower values of Stocks number and Euler number. In the present study, the effect of the curve degree installed at the end of the tangential inlet was investigated in a conventional gas cyclone. Especially, the impact of curve degree on the flow pattern and the gas cyclone performance was investigated numerically for varied inlet velocities by using the turbulent model of RSM. The Eulerian-Lagrangian approach was applied to achieve the distribution of solid particles in different sizes.

2. Government Equations
2.1. Turbulent Modeling
Previous works have been carried out to select an accurate turbulent model since gas flow inside a gas cyclone is complex[5,7,12–26]. They compared turbulent models and then understood that the RSM model is able to evaluate the physical behavior of swirl flow. Hence, such model has been used in simulation to investigate the curve of tangential inlets in gas cyclones. For a constant temperature and incompressible, the usage of equations

DOI: 10.22034/cmes.2024.2024131.1022

in the current study is continuity and balanced momentum.

$$\frac{\partial \overline{u_i}}{\partial x_i} = 0 \quad (1)$$

$$\frac{\partial \overline{u_i}}{\partial t} + \overline{u}_j \frac{\partial \overline{u_i}}{\partial x_j} = -\frac{1}{\rho}\frac{\partial \overline{P}}{\partial x_i} + \nu \frac{\partial^2 \overline{u_i}}{\partial x_i \partial x_j} - \frac{\partial}{\partial x_j} R_{ij} \quad (2)$$

Where $\bar{u}_i$ is the mean velocity vector, x_i is the position vector, $\overline{P}$ is the mean pressure, ρ is the gas density, ν is the gas kinematic velocity, and $R_{ij} = \overline{u_i' u_j'}$ is the Reynolds stress tensor. Here $u_i' = u_i - \overline{u_i}$ is the ith fluctuating velocity component. The RSM turbulence model provides the transport equations for the evaluation of turbulence stresses. That is,

$$\frac{\partial}{\partial t} R_{ij} + \overline{u_k}\frac{\partial}{\partial x_k} R_{ij} = \frac{\partial}{\partial x_k}\left(\frac{\nu_t}{\sigma^k}\frac{\partial}{\partial x_k} R_{ij}\right) - \left[R_{ik}\frac{\partial \overline{u_j}}{\partial x_i} + R_{jk}\frac{\partial \overline{u_i}}{\partial x_k}\right] - C_1 \frac{\varepsilon}{k}\left[R_{ij} - \frac{2}{3}\delta_{ij}K\right] - C_2\left[P_{ij} - \frac{2}{3}\delta_{ij}P\right] - \frac{2}{3}\delta_{ij}\varepsilon \quad (3)$$

Where the turbulence production term P_{ij} is given as,

$$P_{ij} = -\left[R_{ik}\frac{\partial \overline{u_j}}{\partial x_k} + R_{jk}\frac{\partial \overline{u_i}}{\partial x_k}\right], P = \frac{1}{2}P_{ij} \quad (4)$$

Here P stands for the fluctuating kinetic energy production, ν_t stands for the turbulence (eddy) kinematic viscosity, and the empirical constants are $\sigma^k = 1, C_1 = 1.8, C_2 = 0.8$. The transport equation for the turbulence dissipation rate, ε, is given as,

$$\frac{\partial \varepsilon}{\partial t} + \overline{u_j}\frac{\partial \varepsilon}{\partial x_j} = \frac{\partial}{\partial x_j}\left[\left(\nu + \frac{\nu_t}{\sigma^\varepsilon}\right)\frac{\partial \varepsilon}{\partial x_j}\right] - C^{\varepsilon 1}\frac{\varepsilon}{K}R_{ij}\frac{\partial \overline{u_i}}{\partial x_j} - C^{\varepsilon 2}\frac{\varepsilon^2}{K} \quad (5)$$

Where $k = \frac{1}{2}\overline{u_i' u_j'}$ is the fluctuating kinetic energy. The values of constants are $\sigma^\varepsilon = 1.3, \sigma^{\varepsilon 1} = 1.44, \sigma^{\varepsilon 2} = 1.92$.

3. Discrete Particle modeling (DPM)

The governing equation of the solid particle in the gas flow was given as follows:

$$\frac{d\vec{x}_p}{dt} = \vec{u}_p \quad (6)$$

$$\frac{d\vec{u}_p}{dt} = F_D\left(\vec{u} - \vec{u}_p\right) + \vec{a} \quad (7)$$

In Equation (7), the first term on the right-hand side is the drag force in which

$$F_D = \frac{18\mu}{\rho_p {d_p}^2}\frac{C_D Re_P}{24} \quad (8)$$

The second term is the acceleration of gravity including buoyancy given as,

$$\vec{a} = \vec{g}\left(\frac{\rho_p - \rho}{\rho_p}\right) \quad (9)$$

The Saffman force and the virtual mass effect are neglected here. In Equation (8), the particle Reynolds number and the drag coefficient of Schiller and Nauman[27] are, respectively, given by:

$$Re \equiv \frac{\rho d_p |\vec{u}_p - \vec{u}|}{\mu} \quad (10)$$

$$C_D = \begin{cases} \dfrac{24}{\mathrm{Re}_p} & \mathrm{Re}_p < 0.1 \\ \dfrac{24}{\mathrm{Re}_p}\left(1 + 0.15\,\mathrm{Re}_p^{\,0.687}\right) & 0.1 < \mathrm{Re}_p \le 1000 \\ 0.44\,\mathrm{Re}_p & > 1000 \end{cases} \quad (11)$$

The DRW model was used to predict the turbulent dispersion effects. Accordingly, the fluctuation velocity, u_i', during the eddy lifetime, T_e , is estimated by

$$u_i' = \varsigma\sqrt{\overline{u_i' u_i'}} \quad (12)$$

In which $\varsigma$is a zero-mean unit variance normally distributed random number, and $\sqrt{\overline{u_i' u_i'}}$ is the local root mean square (RMS) fluctuation velocity in ith direction. The eddy lifetime is given as,

$$T_e = 2T_L \quad (13)$$

Where T_L is the fluid Lagrangian integral time scale that is estimated by:

$$T_L = C_L\frac{k}{\varepsilon} \quad (14)$$

Where $C_L$is the eddy lifetime constant.

4. Solver sitting and Boundary condition

The detailed numerical schemes employed in the current simulation, include discretization scheme momentum, pressure, turbulent dissipation rate, turbulent kinetic energy, and Reynolds stress. In addition, in the current work, the coupling between velocity and pressure is SIMPLE, which is described in Table 1.

Table1. Numerical strategy for the present work.

Numerical setting	Scheme
Pressure discretization	Body force weighted
Pressure velocity coupling	SIMPLE
Momentum discretization	QUICK
Turbulent kinetic energy	Second-order upwind
Turbulent dissipation rate	Second-order upwind
Reynolds stress	First-order upwind

Uniform velocity is employed at the tangential channel, outflow at the exit tube, and no-slip is applied for all walls. 19.5 m/s is utilized for the inlet velocity. Air density (ρ) and dynamic viscosity (μ) is 1.225 kg/m^3 and 1.7*10^{-5} (Pa.s), respectively. The turbulent intensity (I) corresponds to 5% and the turbulence characteristic length amounts to 0.07 times the channel width.

5. Grid Independent (GI) and Validation

The numerical studies investigated, observing the hydrodynamic of airflow in gas cyclones, which are shown in Table 2 and Fig1.

DOI: 10.22034/cmes.2024.2024131.1022

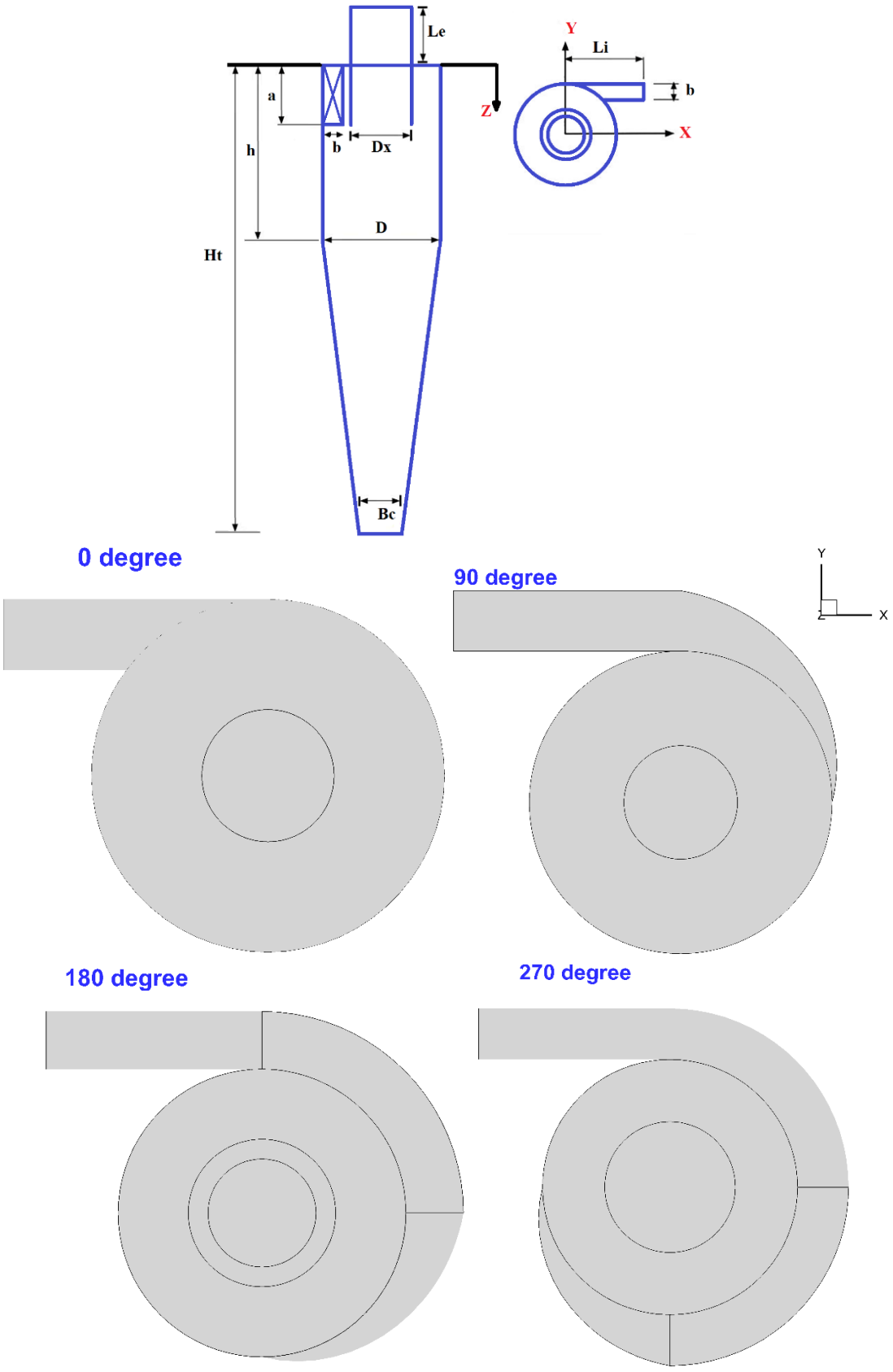

Fig1.Diffrernt models of gas cyclone.

DOI: 10.22034/cmes.2024.2024131.1022

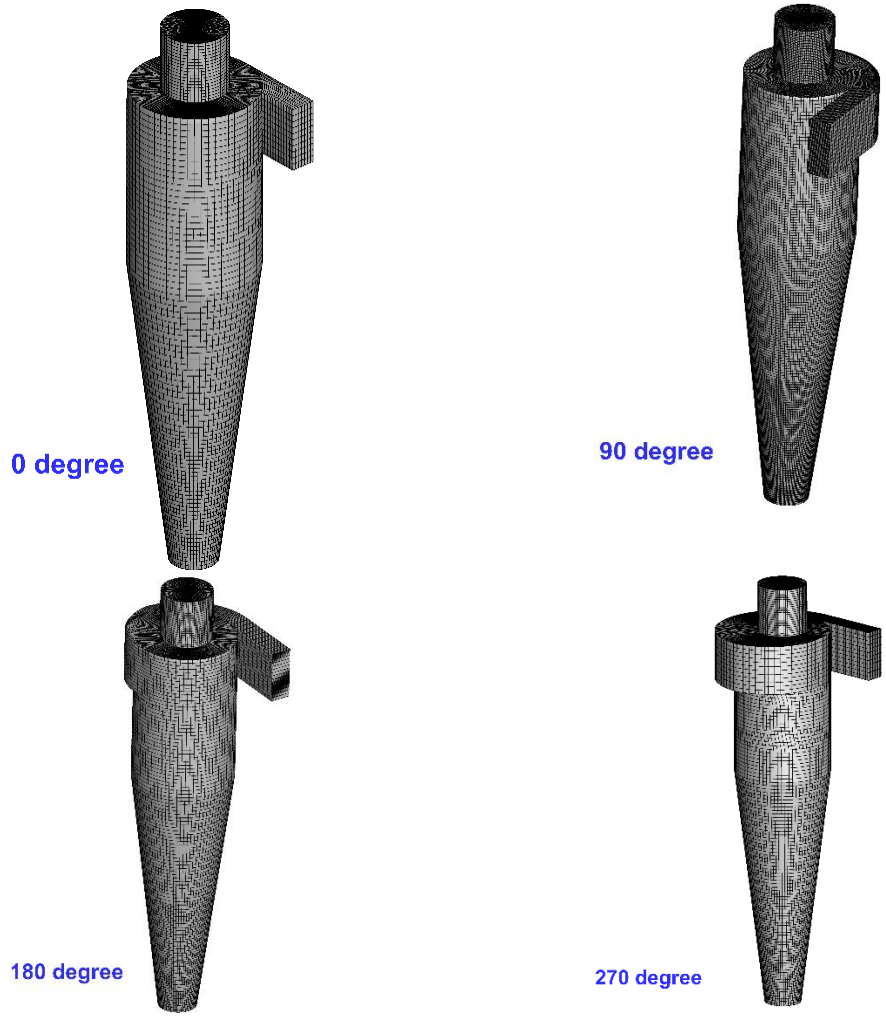

Fig 2. 3D Multi-block Grid.

Table2. Geometrical dimension of gas cyclone.

Dimension	Length (m)	Dimension ratio (Dimension/D)
Body diameter, D	0.205	1
Inlet height, a	0.105	0.5
Inlet width, b	0.041	0.2
Gas outlet diameter, D_x	0.105	0.5
Gas outlet duct length, S	0.105	0.5
Cone-tip diameter, B_c	0.076875	0.375
Cylinder height, h	0.3075	1.5
Cyclone height, H_t	0.82	4
Duct length, L_i	0.15375	0.75
Outlet trube length, L_e	0.1025	0.5

All present gas cyclones generated a multi-black 3-D grid, as illustrated in Fig 2. The mesh independence has been investigated under varied grids, which determine in Table 2 and Fig 3 the trend of tangential velocity.
In this investigation to compare numerical results with experimental data Pressure drop, axial velocity, tangential velocity and collection efficiency use Hoekstra[28] and Zhao[29] as shown in Fig 3.

Table2. Grid independent for the present simulation

Total number of cells	Static pressure drop	Total pressure drop
394700	1355.44	1139.28
455900	1398.90	1159.77
578300	1458.32	1188.48
Difference (%) [a]	7.05	4.1

[a] The percentage difference between the coarsest and the finest grid.

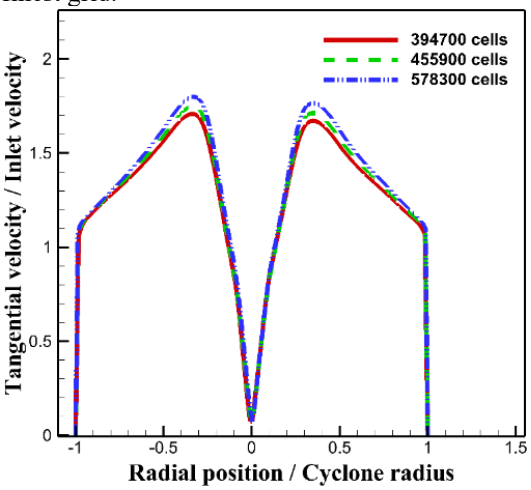

Fig2. Numerical tangential velocity of different meshes (Z=0.75D).

DOI: 10.22034/cmes.2024.2024131.1022

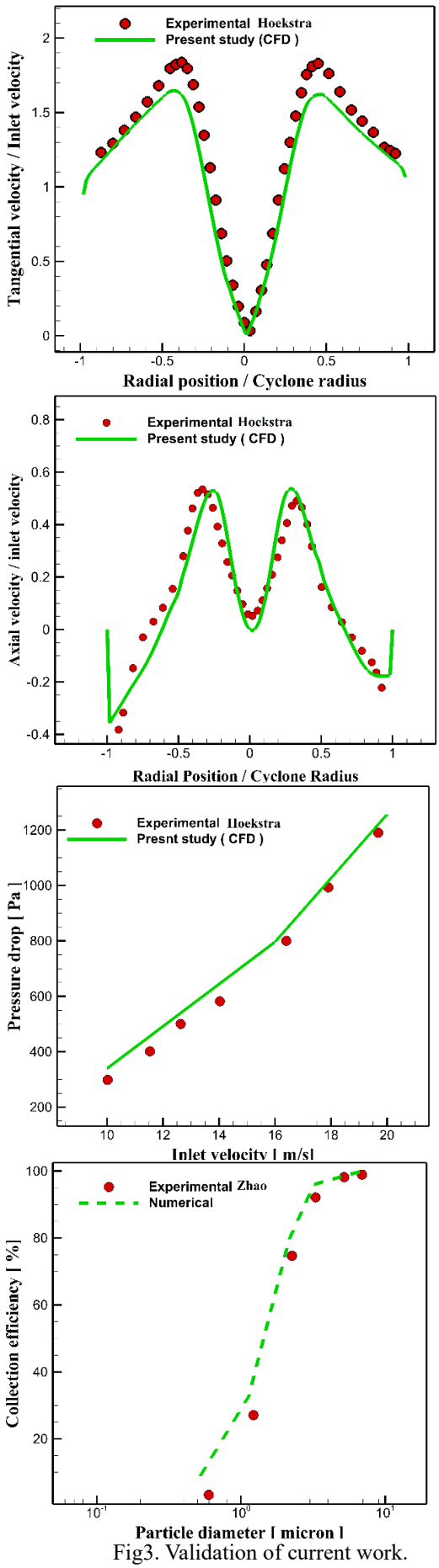

Fig3. Validation of current work.

6. Results

6.1. Tangential velocity

Generally, tangential velocity has led to the centrifugal force, which helps separate solid particles. The tangential velocity distribution consists of two regions called forced vortex and free vortex. The forced vortex starts growing in the central region to reach the tipping point($V_\theta = r\omega$). The free vortex starts decreasing at the tipping point to reach the wall ($V_\theta = \frac{C}{r}$). All tangential velocity sections illustrated fig4.

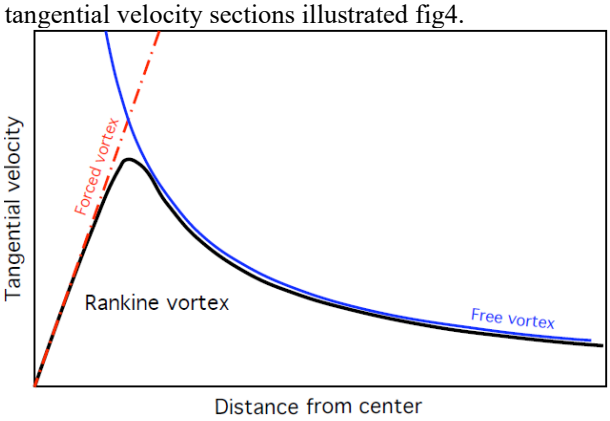

Fig4. Different parts of tangential velocity.

Previous investigations have shown that the tangential velocity pattern changes with the smallest geometry change. In table 3 redial positions have been indicated:

Table3. Radial positions from S_1 to S_9.

Section	Z/D
S_1	0.75
S_2	1.0
S_3	1.25
S_4	1.5
S_5	1.75
S_6	2
S_7	2.25
S_8	2.5
S_9	2.75

As illustrated in Fig5, the angle increasing of the inlet can increase the tangential velocity. The tangential velocity maximum is between 1.8 to 2 m/s and the shape of the flow pattern is a V shape, on the other hand, close to the walls, the amount of tangential velocity is 1.1 to 1.3 it has been indicated that applying an inlet curve can affect tangential velocity as well as such inlet curves can lead to increasing primary acceleration that may improve collection efficiency.

As illustrated in Fig6, minimum of tangential velocity occurs in center of gas cyclone. However, increasing of tangential velocity is growing close to walls that has been indicated that airflow has high swirl flow in all walls.

DOI: 10.22034/cmes.2024.2024131.1022

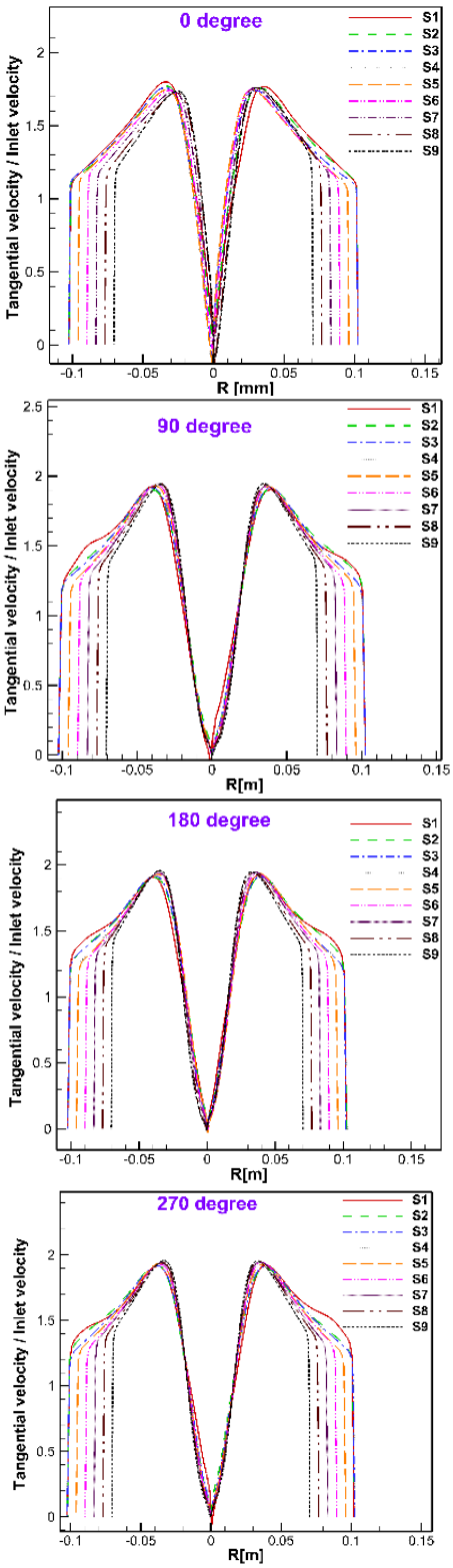

Fig5. Distribution of tangential velocity in different positions.

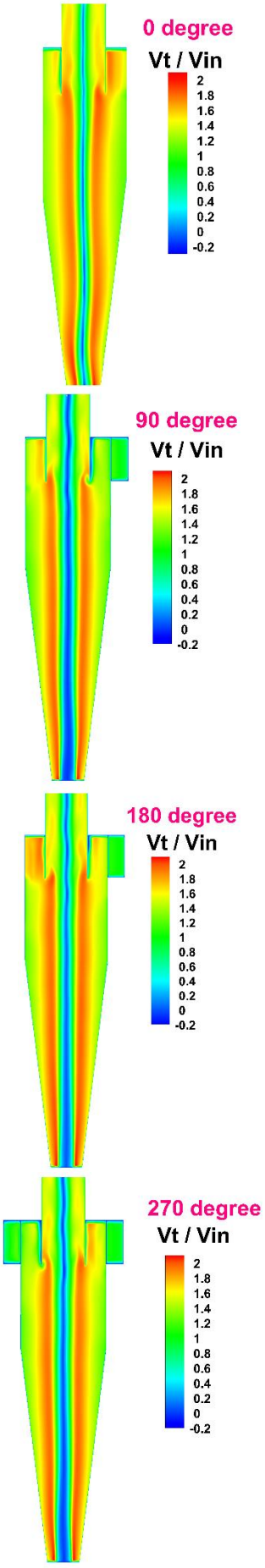

Fig6. Tangential velocity contours (V=19.5m/s).

DOI: 10.22034/cmes.2024.2024131.1022

6.2. Axial velocity

In gas-solid separators, the axial velocity has a key role in making easy the movement of solid particles nearby the wall. The separator's axial flow is made up of two main regions: upward flow that is mainly comprised of airflow with some solid particles, and the downward flow come across near walls, including mixture of particles and gas. Such behavior is illustrated in fig7.

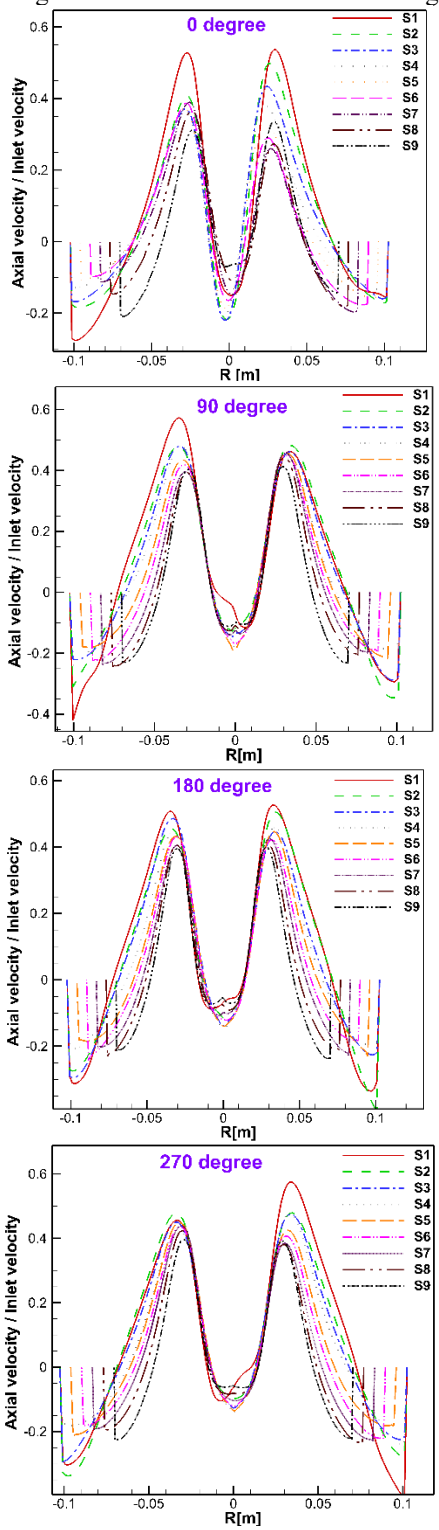

Fig7. Axial velocity in different lines.

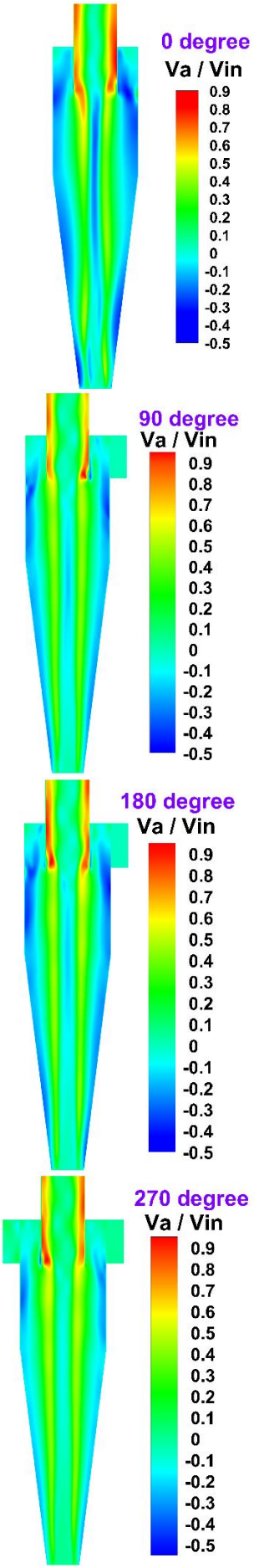

Fig8.Axial velocity contours (V=19.5m/s)

DOI: 10.22034/cmes.2024.2024131.1022

Fig8 shows dimensionless axial velocity contour plot for varied curves with gas velocity 19.5 m/s. It has been observed that axial velocity is negative in the wall region that solid particles move up inward, however axial velocity is positive in the core, where fine particles move to exit tube and then escape via vortex finder. Maximum of axial velocity is located in vortex finder region than other parts. Installing a curve at the end of the tangential inlet can stabilize the vortex end in the conical part which can improve collection efficiency and more particles are trapped.

6.3. Pressure drops

One of the vital factors, which can greatly influence the gas cyclone performance, is pressure drop. The pressure drop inside gas cyclones results from factors, including the frictional surface, the expansion gas, the rotational kinetic energy and vortex. Generally, the amount of pressure drop calculated the difference of outlet and inlet. As is illustrated in fig9, installing inlet curve can affect pressure drop and lead to increasing of negative pressure in central and also, amount of pressure drop decrease nearby walls.

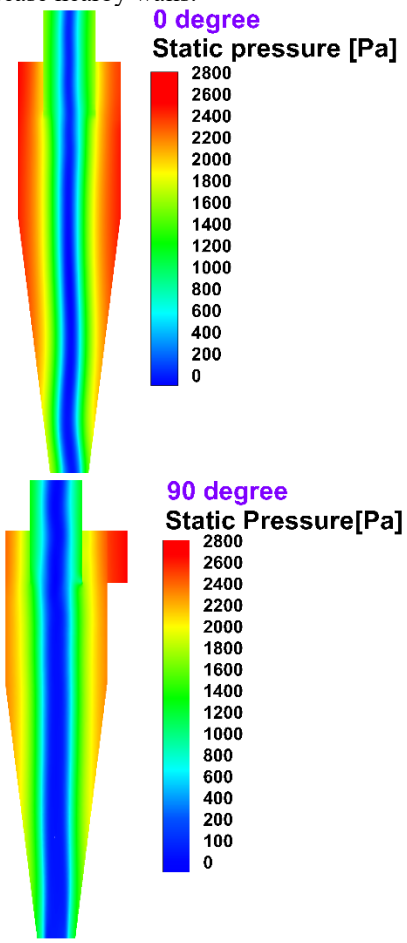

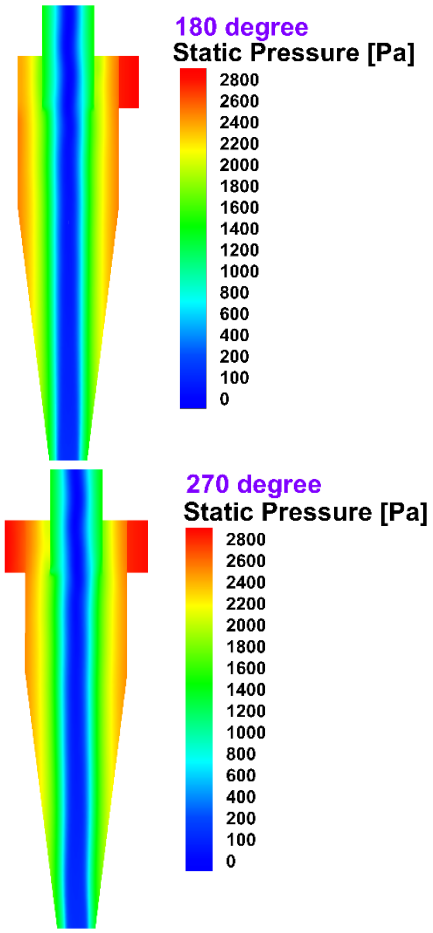

Fig9. Distribution of pressure drop (V=19.5 m/s).

Fig. 10 illustrates that increasing of curve degree affect pressure drop. As been shown that increasing of curve degree decreases pressure drop and by increasing inlet velocity amount of pressure drop increases at varied curves also it is clearly seen that conventional gas cyclone has higher-pressure drop in comparison to other gas cyclones. To sum up, the obtained results show that pressure drop severely is related to inlet velocity and geometry.

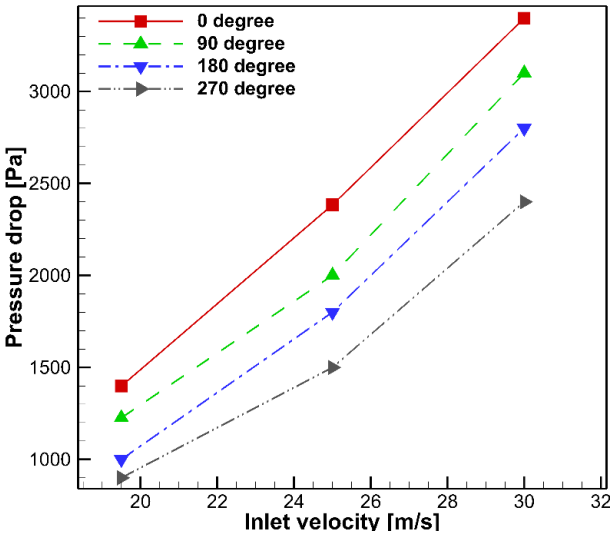

Fig10. Comparability to pressure drop at varied inlet velocity for different designs.

DOI: 10.22034/cmes.2024.2024131.1022

6.4. *Collection efficiency*

The collection efficiency is a significant factor that applied to demonstrate how to separate solid particles from gas. This was defined as η, as follow:

$$\eta = \left(1 - \frac{n_{out}}{n_{in}}\right) \times 100 \quad (15)$$

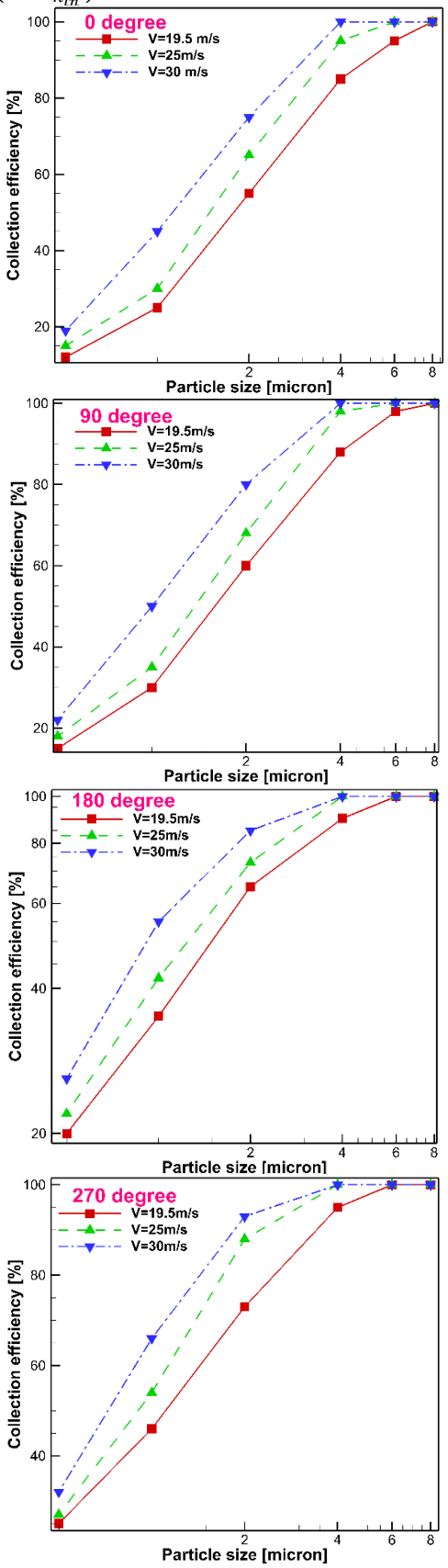

Fig11. Collection efficiency for different gas cyclones.

In Equation of 15, n_{out} and n_{in} are the number of inlet and outlet particles, respectively. as is illustrate in fig11, the collection efficiency increases as size of particles increase and also distribution of it has a form of S shape. Moreover, with increasing inlet velocity, the collection efficiency increases. Installing an inlet curve at the end part can rise acceleration of gas and particle and lead to increase centrifugal force that can improve the collection efficiency than a conventional gas cyclone.

7. Conclusion

The current study investigated airflow inside several conventional gas cyclones, which placed curves of 0-270 degrees at the end of the channel. The RSM model was applied in all cases and DPM was used to evaluate collection efficiency. The obtained resulted are as follows:

1-Increasing inlet velocity leads to the development of collection efficiency and an increase in pressure drop.

2- The usage of the curve can enhance vortex behavior, namely, the vortex is stable and the pattern of tangential velocity is axisymmetric also maximum tangential velocity is almost 1-to-2-time inlet velocity.

3- Using a curve can increase negative pressure at the central and decrease energy loss near walls.

4- Curves, which are installed at the end of the tangential channel led to a stable end vortex at the conical part in the axial velocity contour. In addition, maximum axial velocity is in the exit tube.

In the present work, RSM model used to simulate airflow in gas cyclones that install curves in different angles 0 to 270 degree. The Eulerian-lagrangian approach used to estimate the collection efficiency under varied geometries and their results may be drawn:

1-the form of tangential velocity is M shape and amount of tangential velocity 1.2-to-1.5-time inlet velocity close to walls. Also increasing of curve angle can lead to decrease of tangential velocity in central

2-the shape of axial velocity is inverting W and increasing of curve angle can lead to increase velocity in central in the part of upward flow and creation of curve inlet at end of tangential channel cause stabilization of vortex end in the part of cone that can improve collection efficiency

3- Installing of curve can decrease pressure drop in all walls than a conventional gas cyclone.

4- Increasing of inlet velocity and size of particle lead to improving collection efficiency and trend of particle distribution is S shape roughly.

References

[1] J. Gimbun, CFD Simulation of Aerocyclone Hydrodynamics and Performance at Extreme Temperature, Eng. Appl. Comput. Fluid Mech. 2 (2008) 22–29. https://doi.org/10.1080/19942060.2008.11015208.

[2] X. Gao, J. Chen, J. Feng, X. Peng, Numerical investigation of the effects of the central channel on the flow field in an oil–gas cyclone separator, Comput. Fluids. 92 (2013) 45–55. https://doi.org/10.1016/j.compfluid.2013.11.001.

[3] A. Raoufi, M. Shams, M. Farzaneh, R. Ebrahimi, Numerical simulation and optimization of fluid flow in cyclone vortex finder, Chem. Eng. Process. Process Intensif. 47 (2008) 128–137. https://doi.org/10.1016/j.cep.2007.08.004.

[4] L.S. Brar, R.P. Sharma, R. Dwivedi, Effect of vortex finder diameter on flow field and collection efficiency of cyclone separators, Part. Sci. Technol. 33 (2015) 34–40. https://doi.org/10.1080/02726351.2014.933144.

[5] F. Parvaz, S.H. Hosseini, G. Ahmadi, K. Elsayed, Impacts of the vortex finder eccentricity on the flow pattern and performance of a gas cyclone, Sep. Purif. Technol. 187 (2017) 1–13.

[6] F. Parvaz, S.H. Hosseini, A.R. Bastan, J. Foroozesh, N.U. Babaoğlu, K. Elsayed, G. Ahmadi, Influence of gas exhaust geometry on flow pattern , performance , and erosion rate of a gas cyclone, 40 (2023) 1–11. https://doi.org/10.1007/s11814-023-1430-2.

[7] F. Parvaz, S.H. Hosseini, A.R. Bastan, J. Foroozesh, N.U. Babaoğlu, K. Elsayed, G. Ahmadi, Influence of gas exhaust geometry on flow pattern, performance, and erosion rate of a gas cyclone, Korean J. Chem. Eng. 40 (2023) 1587–1597. https://doi.org/10.1007/s11814-023-1430-2.

[8] F. Qian, Y. Wu, Effects of the inlet section angle on the separation performance of a cyclone, Chem. Eng. Res. Des. 87 (2009) 1567–1572. https://doi.org/10.1016/j.cherd.2009.05.001.

[9] F.P. Qian, M.Y. Zhang, Effects of the inlet section angle on the flow field of a cyclone, Chem. Eng. Technol. Ind. Chem. Equipment-Process Eng. 30 (2007) 1564–1570.

[10] H. Safikhani, J. Zamani, M. Musa, Numerical study of flow field in new design cyclone separators with one , two and three tangential inlets, Adv. Powder Technol. (2017). https://doi.org/10.1016/j.apt.2017.12.002.

[11] A.L. Liu, Y.H. Zhang, L. Ma, Y.M. Wang, M.Y. He, Effect of inlet particle arrangement on separating property of a cyclone separator, Korean J. Chem. Eng. 35 (2018) 1380–1387. https://doi.org/10.1007/s11814-018-0026-8.

[12] N.U. Babaoğlu, F. Parvaz, S.H. Hosseini, K. Elsayed, G. Ahmadi, Influence of the inlet cross-sectional shape on the performance of a multi-inlet gas cyclone, Powder Technol. 384 (2021) 82–99. https://doi.org/10.1016/j.powtec.2021.02.008.

[13] F. Parvaz, S.H. Hosseini, K. Elsayed, G. Ahmadi, Influence of the dipleg shape on the performance of gas cyclones, Sep. Purif. Technol. 233 (2020) 1–14. https://doi.org/10.1016/j.seppur.2019.116000.

[14] E. Dehdarinejad, F. Parvaz, S.H. Hosseini, G. Ahmadi, K. Elsayed, To, Performance analysis of a gas cyclone with a dustbin inverted hybrid solid cone, Aerosol Sci. Technol. ISSN. 56 (2023) 587–599. https://doi.org/10.1016/j.cherd.2023.04.012.

[15] E. Dehdarinejad, M. Bayareh, F. Parvaz, S.H. Hosseini, G. Ahmadi, Performance analysis of a gas cyclone with a converging-diverging vortex finder, Chem. Eng. Res. Des. 193 (2023) 587–599. https://doi.org/10.1016/j.cherd.2023.04.012.

[16] J. Foroozesh, F. Parvaz, S.H. Hosseini, G. Ahmadi, K. Elsayed, N.U. Babaoğlu, Computational fluid dynamics study of the impact of surface roughness on cyclone performance and erosion, Powder Technol. 389 (2021) 339–354. https://doi.org/10.1016/j.powtec.2021.05.041.

[17] M. Izadi, A.M. Makvand, E. Assareh, F. Parvaz, Optimizing the Design and Performance of Solid-Liquid Separators, Int. J. Thermofluids. 5–6 (2020) 100033. https://doi.org/10.1016/j.ijft.2020.100033.

[18] K. Elsayed, F. Parvaz, S.H. Hosseini, G. Ahmadi, Influence of the dipleg and dustbin dimensions on performance of gas cyclones: An optimization study, Sep. Purif. Technol. 239 (2020) 116553.

[19] F. Parvaza, Seyyed Hossein Hosseini, Goodarz Ahmadic, Khairy Elsayed, Impacts of the vortex finder eccentricity on the flow pattern and performance of a gas cyclone, Sep. Purif. Technol. 63 (2004) 1–11.

[20] N.U. Babaoğlu, K. Elsayed, F. Parvaz, J. Foroozesh, S.H. Hosseini, G. Ahmadi, Analysis and optimization of louvered separator using genetic algorithm and artificial neural network, Powder Technol. 398 (2022) 117077. https://doi.org/https://doi.org/10.1016/j.powtec.2021.117077.

[21] Nihan Uygur Babao˘glu, F. Parvaz, J. Foroozesh, S. Hossein, Geometry optimization of axial cyclone for high performance and low acoustic noise, 427 (2023). https://doi.org/10.1016/j.powtec.2023.118738.

[22] S.M. Vahedi, F. Parvaz, R. Rafee, M.K. Bakavoli, Journal of Heat and Mass Transfer Research Computational fluid dynamics simulation of the flow patterns and performance of conventional and dual-cone gas-particle cyclones, 4 (2018) 27–38. https://doi.org/10.22075/jhmtr.2017.1503.1100.

[23] S.M. Vahedi, F. Parvaz, M. Khandan Bakavoli, M. Kamali, Surface roughness effect of on vortex length and efficiency of the gas-oil cyclone through CFD modelling, Iran. J. Oil Gas Sci. Technol. 0 (2018) 68–84. https://doi.org/10.22050/ijogst.2018.102377.1417.

[24] F.Parvaz, R.Rafee, F.Tallebi, Effects of the Outlet Pipe Diameter on the Performance of Aerocyclone in Gas Droplet Two-Phase Flow, J. Mech. Eng. 48 (2018) 45–53.

[25] Abdali A, Monjezi V. Machine Learning-based Flexible Link Robot Control. Computational methods in engineering sciences. 2023 Aug 23;1(2):12-7.

[26] Azizi A, Toohidinejad Z, Haghighatpoor I. Design and analysis of adaptive control of the reference model to control the output pressure of the boiler system. Computational methods in engineering sciences. 2023 May 22;1(1):21-6.

[27] Z. Naumann, L. Schiller, A drag coefficient correlation, Z. Ver. Deutsch. Ing. 77 (1935) e323.

[28] A.J. Hoekstra, Gas flow field and collection eficiency od cyclone seperators., (2000).

[29] B. Zhao, Development of a new method for evaluating cyclone efficiency, Chem. Eng. Process. Process Intensif. 44 (2005) 447–451. https://doi.org/10.1016/j.cep.2004.06.007.